

Hopkins Ultraviolet Telescope Observations of Her X-1

Bram Boroson

Center for Astrophysics, 60 Garden Street, Cambridge, MA 02138; bboroson@cfa.harvard.edu

William P. Blair, Arthur F. Davidsen

Department of Physics and Astronomy, The Johns Hopkins University, Charles & 34th Streets,
Baltimore, MD 21218; wpb@pha.jhu.edu, afd@pha.jhu.edu

S.D. Vrtilek, John Raymond

Center for Astrophysics, 60 Garden Street, Cambridge, MA 02138; svrtilek@cfa.harvard.edu,
jraymond@cfa.harvard.edu

Knox S. Long

Space Telescope Science Institute, 3700 San Martin Drive, Baltimore, MD 21218; long@stsci.edu

and

Richard McCray

JILA, Campus Box 440, University of Colorado, Boulder, CO 80309; dick@jila.colorado.edu

ABSTRACT

We have obtained a far-ultraviolet spectrum of the X-ray binary Hercules X-1/HZ Herculis using the Hopkins Ultraviolet Telescope aboard the Astro-1 space shuttle mission in 1990 December. This is the first spectrum of Her X-1 that extends down to the Lyman limit at 912 Å. We observed emission lines of O VI $\lambda\lambda$ 1031.9, 1037.6, NV $\lambda\lambda$ 1238.8, 1242.8, and CIV $\lambda\lambda$ 1548.2, 1550.8, and the far UV continuum extending to the Lyman limit. We examine the conditions of the emitting gas through line strengths, line ratios, and doublet ratios. The UV flux is lower by about a factor of 2 than expected at the orbital phase of the observation. We model the UV continuum with a simple power-law and with a detailed model of an X-ray-illuminated accretion disk and companion star. The power-law provides a superior fit, as the detailed model predicts too little flux below 1200 Å. We note, however, that there are uncertainties in the interstellar reddening, in the background airglow spectrum, and in the long-term phase of the accretion disk. We have searched the data for UV line and continuum pulsations near the neutron star spin period but found none at a detectable level.

Subject headings: ultraviolet: stars, stars: individual (HZ Her), stars: binaries: close, stars: neutron

1. Introduction

Hercules X-1/HZ Herculis is a low mass X-ray binary system consisting of a $\approx 1.3 M_{\odot}$ neutron star and a $\approx 2.2 M_{\odot}$ A dwarf star locked in orbit about each other with a period of 1.7 d (Deeter et al. 1991, and references therein). The X-ray source is eclipsed by the A star for 0.24 d of each period, indicating an orbital inclination near 90° . The spectral type of the A star varies with orbital phase from late B/early A to late A/early F such that the later spectral types correspond to eclipse and the earlier spectral types correspond to 1/2 an orbit later (when X-ray heating of the A star should be most apparent—see Milgrom & Salpeter 1975). Mass transfer, which may be periodic, feeds an accretion disk around the neutron star. Accretion onto the neutron star itself, which has a magnetic field of $\sim 4 \times 10^{12}$ Gauss, occurs on the magnetic poles (Gruber et al. 1980; Voges et al. 1982).

The X-rays from the system vary on a period near 34.85 d (Ögelman 1987, Baykal et al. 1993), with an X-ray high state typically lasting ≈ 11 d, and an X-ray low state (with a secondary maximum of 30% the high state) lasting ≈ 24 d. The time at which the X-ray high state begins varies unpredictably from the mean ephemeris by more than ± 1 d, an effect that has led to the generation of a number of different models (e.g. Petterson 1975; Gerend & Boynton 1976; Wolff & Kondo 1978; Kondo, Van Flandren, & Wolff 1983; Meyer & Meyer-Hofmeister 1984; Schandl & Meyer 1994). As the 1.7 day modulation of the optical light continues during the X-ray low states (Bahcall & Bahcall 1972), the 35-day cycle probably results from a geometric effect, such as obscuration by a precessing accretion disk, and not an interruption of the accretion, which would cause the X-ray heating of HZ Her to cease. In addition to the 35 d cycle, pulsed X-ray emission with a period of 1.24s is also seen, which is generally interpreted as the rotation period of the neutron star (Tananbaum et al. 1972; Giacconi et al. 1973). These pulsations have also been detected optically (Davidsen et al. 1972; Middleditch 1983), in the UV (Borson et al. 1996) and at optical and infrared wavelengths (Middleditch, Puetter, & Pennypacker 1985).

The ultraviolet spectrum above 1200 \AA has been extensively observed with IUE (Dupree et al. 1978; Gursky et al. 1980; Howarth & Wilson 1983a,b; Vrtilik & Cheng 1996). Both the line and continuum components of the spectrum vary with orbital phase. The ultraviolet light from Her X-1 comes from at least two main regions within the system: the heated face of the normal star and the accretion disk. According to the analysis of Howarth & Wilson (1983a), roughly 1/2 of the hard X-rays striking the A star are reprocessed into UV and optical continuum emission. Reprocessed X-rays are also responsible for most of the UV light from the disk. Using the Goddard High Resolution Spectrograph (*GHR*S) aboard the Hubble Space Telescope, Borson et al. (1996) showed that the UV lines have broad and narrow components which they interpreted in terms of emission from the disk and the star.

In this paper, we present a spectrum of Her X-1 that extends the far-ultraviolet wavelength coverage to the Lyman limit at 912 \AA . We have detected, for the first time, the O VI $\lambda\lambda 1031.9, 1037.6$ emission lines, and the continuum in this wavelength region. In §2 we

discuss the observations and data reduction, and in §3 we discuss our data in the context of other observations of Her X-1, and we compare the data with models of the line and continuum emission.

2. Observations

The observations were carried out with the Hopkins Ultraviolet Telescope (HUT) as part of the Astro-1 space shuttle mission in 1990 December. HUT consists of a 0.9 m mirror that feeds a prime focus spectrograph with a microchannel plate intensifier and reticon detector. First order sensitivity covers the region from 850 Å to 1850 Å at 0.51 Å pix⁻¹, with ≈3Å resolution. The detector can be operated in any of several modes, including a high time resolution mode where individual photons can be time-tagged to a relative accuracy of 1 ms and an absolute accuracy of 3 ms. This was the mode of operation during the observation described here. Further details of the spectrograph and telescope and their on-orbit performance and calibration can be found in Davidsen et al. (1992) and Kruk et al. (1997).

The Her X-1 observation discussed here took place on 1990 December 6 at 4:22 UT. According to the 1.7 day orbital ephemeris of Deeter et al. (1991), this corresponds to $\phi_{\text{orb}} = 0.66$. We do not know the X-ray state of Her X-1 at the time of our observation. Using a period $P_{35} = 34.9$ d and the observed X-ray turn-on nearest in time to our observation (JD 2448478.3, as given in Baykal et al. 1993), our observation took place at $\phi_{35} = 0.93$, while X-ray turn-on occurs at $\phi_{35} = 0.0$. This suggests that our observation took place in the X-ray off state; however, the times of the X-ray turn-ons are known to vary by ~6 days (Ögelman 1987; Baykal et al. 1993), so that without simultaneous X-ray observations, we can not be certain.

The HUT observation was made with an 18" aperture placed on the object, and guiding was accomplished using preplanned guide star positions on the HUT TV guider. The total integration was 1700 s. Orbital viewing constraints required that we observe Her X-1 entirely during the orbital day of HUT, which resulted in substantial airglow contamination, leading not only to significant line emission (including several EUV lines seen in second order) but also a pseudo-continuum from grating-scattered light (chiefly from the brightest airglow lines at Ly α and O I λ 1302).

The flux calibration is based on observations of the white dwarf star G191-B2B compared with model stellar atmospheres and laboratory calibrations as discussed by Davidsen et al. (1992) and Kruk et al. (1997). The relative fluxes are accurate to within 5%.

The count rate in the continuum from Her X-1 (in the 1400–1600Å range, relatively free from airglow emission) was not uniform, but peaked at 5.5 counts s⁻¹ during a five-minute interval. This count rate should be compared with an average rate of 4.3 counts s⁻¹ (1400–1600Å) in the 1500 s interval that we used for our analysis. Data from the HUT TV camera indicate sections at the beginning and end of the observation where pointing stability was disrupted. Post-flight analysis of video frames stored during the observation show that even during the portion of the

observation where the pointing stability was good, the object was not well centered in the slit, especially in the coordinate perpendicular to the dispersion direction. Hence, even minor pointing errors could have affected the count rate (and derived flux) because of vignetting by the edge of the slit. (The PSF of the telescope produced star images with $\text{FWHM} \sim 5''$.) We thus suspect that the fluctuating count rate was due to pointing errors, and that the maximum observed count rate is probably representative of the true flux of the object. This analysis implies that the average count rate was low by $\approx 27\%$; the derived fluxes (and errors) were thus multiplied by 1.27 to correct for this effect. Since the HUT detector is photon-counting, it is straightforward to generate and propagate errors along with the data as various operations are performed. To the extent that flux was being lost even during stable pointing (due to vignetting) this corrected flux could still be too low, but not by more than $\sim 20\%$. The corrected, flux-calibrated spectrum is shown as the upper curve in Figure 1.

In order to subtract airglow contamination to first order, we have fit and subtracted a blank day sky observation obtained with the same aperture during Astro-1. We used smooth fits to the known airglow lines in this spectrum instead of the observed airglow background to reduce the contribution of counting noise. An actual smoothing of the background spectrum, instead of a fit to individual lines, would have increased the widths of the strong airglow lines where they overlap emission lines from Her X-1. We have continued to use the error array associated with the counts in the original data. The result of our fit to the background spectrum is shown as the lower curve in Figure 1.

The airglow-subtracted spectrum representing the summed intrinsic data from the source is shown in Figure 2. Because the relative intensities of the fainter airglow lines change with orbital latitude and look-angle with respect to the earth limb, the subtraction of line emission is not perfect. Also, a variable complex of airglow emissions affects the spectrum in the region near the Lyman limit (cf. Feldman et al. 1992). However, our technique should be sufficient to provide a reasonable representation of the intrinsic continuum longward of 930 \AA . This is the spectrum that will be used for continuum fitting below.

We have identified emission from the $\text{NV } \lambda\lambda 1238.8, 1242.8$ doublet and the $\text{CIV } \lambda\lambda 1548.2, 1550.8$ doublet, which have been seen with IUE (Boyle et al. 1986, Howarth & Wilson 1983a, 1983b) and HST (Anderson et al. 1994; Boroson et al. 1996), and also the $\text{OVI } \lambda\lambda 1031.9, 1037.6$ resonance doublet and some fainter emission lines at a more marginal detection level. This constitutes the first detection of O VI emission from the Her X-1 system, and provides a significant new diagnostic of photoionized gas in this system.

In order to provide quantitative estimates of the line strengths, we have fit Gaussian profiles to the data. Since some of the lines, including $\text{OVI } \lambda\lambda 1031.9, 1037.6$, are affected by nearby airglow features, we first used our template airglow spectrum to carry out a local subtraction of the airglow in order to produce a flat continuum adjacent to each line. Typically, this required us to scale the template spectrum by of order 20% from the value used above to achieve a reasonable

local fit near the lines.

Each doublet was fit assuming an optically thick 1:1 ratio for the lines and a fixed separation of the doublet components (although the central wavelength of each feature was allowed to vary). Observations with the HST show two line components; for a narrow component, the doublet ratios are typically $\approx 1.3 : 1$, while for the broad component, the doublet ratio is more nearly $1 : 1$. We found a superior fit (reduced $\chi^2 = 1.51$ instead of $\chi^2 = 1.73$ with 42 degrees of freedom) when we allowed a $2 : 1$ doublet ratio for O VI $\lambda\lambda$ 1031.9, 1037.6. Allowing the doublet ratio to be a free parameter does not improve the fit ($\chi^2 = 1.52$ for a ratio of 1.65:1). Alternately, the O VI $\lambda\lambda$ 1031.9, 1037.6 lines could have a 1:1 ratio, but an interstellar C II λ 1037.3 line could absorb O VI λ 1037.6. Allowing the wavelength of the interstellar line to vary, but fixing its width as the width of the O VI lines (the instrumental width), we found $\chi^2 = 1.57$ with 42 degrees of freedom. The χ^2 value for all the O VI fits may be artificially high, as the errors do not reflect the uncertainty in the subtraction of the nearby strong airglow lines of H Ly β , O I λ 1026, and O I λ 1040. Figure 3 shows the region near O VI $\lambda\lambda$ 1031.9, 1037.6 with the observed and modelled airglow lines, and Figure 4 shows the best fits for all the lines.

In addition to O VI $\lambda\lambda$ 1031.9, 1037.6, N V $\lambda\lambda$ 1238.8, 1242.8, and C IV $\lambda\lambda$ 1548.2, 1550.8, there was marginal (3σ) evidence for an O V line at 1371 Å, at a strength relative to N V and C IV similar to that seen with the HST. He II λ 1640 may also have been detected at a marginal level. There is no evidence for Si IV λ 1400, and while some features appear at ≈ 974 Å, they are not significant enough to identify as C III λ 977. Any possible C III λ 1176 is lost in the airglow emission that affects this region of the spectrum.

All of the lines intrinsic to Her X-1 are blueshifted. After detailed inspection of the video frames, we were unable to determine unequivocally whether or not this shift is real. Based on analysis of two guide stars, we infer an offset within the aperture in the dispersion direction that is consistent with a blueshift of $0.0 - 1.9$ Å ($0.0 - 5.6''$ miscentering). The discrepant results from the different guide stars are due to a combination of distortions within the TV camera and measurement error. If the blueshift caused by the miscentering is near 1.9 Å, then the apparent blueshifts of the lines are not real, and it becomes more likely that interstellar C II λ 1037.3 can absorb O VI λ 1037.6.

We searched for pulsations in the UV lines from Her X-1, using the data as received in high time rate mode during the time period 1990 Dec 6 04:29:00 to 04:48:20 (UT). We added counts in 0.2 s intervals, folded the data over several likely pulsation periods near the neutron star rotation period, and applied the Analysis of Variance method (ANOVA, Davies 1990) to determine the likelihood of pulsations. No significant pulsations were found in the lines or continuum. However, due to the low count rate and the extensive airglow contamination, the limits on pulsation amplitude, $15 - 35\%$ of the total flux, are not stringent.

3. Discussion

3.1. Comparison with Previous Observations

The detection of O VI in Her X-1 is important, but with a single observation at a particular ϕ_{orb} and ϕ_{35} , we are limited in the conclusions we can draw about the system. In this section we discuss the HUT observation in the context of the more extensive IUE and HST spectroscopy of Her X-1.

Howarth & Wilson (1983a,b; hereafter HWA and HWb) discuss a consistently reduced set of IUE data on Her X-1 that cover a range in both orbital period and the 35 day X-ray cycle. The line and continuum strengths show a clear dependence on orbital phase (Figure 3 of HWA displays the 1500 Å continuum and Figure 2 of HWb displays the NV and CIV line strengths). Her X-1 has shown similar line strengths at corresponding orbital phases in subsequent HST observations (Anderson et al. 1994, Boroson et al. 1996) and IUE observations (Vrtilek & Cheng 1996). Plotting the HUT data on Figure 3 of HWA, Figure 2 of HWb, and Figure 5 of Vrtilek & Cheng demonstrates that the HUT fluxes are about a factor of 2 lower than those observed with IUE at phase 0.34/0.66 (i.e. 0.34 from mid-eclipse). Inspection of optical magnitudes provided by the American Association of Variable Star Observers (AAVSO) shows that the 1.7 day optical modulation continued during the period surrounding our observation (V magnitudes $V = 13.1$ at $\phi_{\text{orb}} = 0.40$ and 0.61 , and $V = 14.1$ at $\phi = 0.98$). As X-ray heating is thought to cause both the optical modulation and the UV emission, this suggests that the decrease in UV flux that we observed was a short-lived phenomenon or unrelated to X-ray heating. From our examination of the data we are confident that the decrease is not due to any known shortcoming of the data acquisition and reduction.

3.2. Analysis of the UV Continuum

In addition to the line fits described in §2, we have produced fits to the continuum after airglow subtraction. The continuum spectrum below $\approx 1200\text{\AA}$, reported here for the first time, is important because the accretion disk should contribute more to the continuum flux at shorter wavelengths.

In fitting the continuum, we used regions free of strong airglow emission lines. We chose to fit the continuum with 1) a power law plus extinction component, and 2) a model of an X-ray illuminated accretion disk and Roche lobe-filling star. These fits will be described briefly below.

For the power law fit, we specified initial guesses at a normalization, A (the flux at 1000 Å), and the exponent of the power law, α , so that $F = A(\lambda/1000)^{-\alpha}$. We also applied a Seaton (1979) galactic extinction law, extrapolated to the Lyman limit in a manner that is consistent with Voyager measurements (Longo et al. 1989). For the Her X-1 HUT spectrum, we find $A = 1.3 \pm 0.3 \times 10^{-13} \text{ erg s}^{-1} \text{ cm}^{-2} \text{ \AA}^{-1}$, $\alpha = 1.33 \pm 0.17$, and $E(B - V) = 0.09 \pm 0.02$. The

reduced χ^2 for this fit was 1.17 (with 1125 points and three free parameters). The $E(B - V)$ value is inconsistent with UV observations of the 2200 Å feature (Gursky et al. 1980). Setting $E(B - V) = 0.05$, we find $A = 8.3 \pm 0.2 \times 10^{-14}$ and $\alpha = 0.99 \pm 0.06$. This fit is nearly as good (the reduced χ^2 is still 1.17) as the fit with $E(B - V)$ as a free parameter. We plot this latter model against the data in Figure 5.

We also tried fitting the HUT spectrum with a detailed physical model of an X-ray illuminated accretion disk and star (assumed to fill its Roche lobe). The model is identical to that presented by Cheng, Vrtillek, & Raymond (1995), except that we have used Kurucz model atmospheres (Kurucz 1992) instead of our library of stellar spectra, which does not extend to the Lyman limit. The model solves for the temperature structure of the disk using the method described by Vrtillek et al. (1990), and includes X-ray heating of the normal star, the eclipse of the star by the disk, and the X-ray shadow of the disk on the surface of the normal star using the methods described in Hwa. We used values for the fixed parameters describing Her X-1 given in Table 2 of Cheng et al. (1995), including $E(B - V) = 0.0$.

In Figure 5 we compare the continuum spectrum produced by the detailed disk model with the power-law fit and with the spectrum observed with HUT. The disk contributes $\sim 10\%$ of the optical flux, $\sim 15\%$ of the flux near 1200Å, $\sim 25\%$ of the flux near 1100Å, and $\sim 50\%$ of the flux near 950Å.

The only free parameter in the model is \dot{M} , the mass transfer rate onto the neutron star. The best-fit value for \dot{M} is $\log_{10} \dot{M} = -8.74 \pm 0.01$ (in units of solar masses per year). This value of \dot{M} is lower than the values reported by Vrtillek & Cheng (1996) during an “anomalous low” state of Her X-1 (in their final fit, the lowest value is $\log \dot{M} = -8.68$). With \dot{M} fixed at the best-fit value, the model predicts $V = 13.6$ also at $\phi = 0.41, 0.61$, when AAVSO observers report $V = 13.1$.

The fit of the detailed model is worse than the simple power-law; we find a reduced χ^2 of 1.64. The fit is especially poor below 1200Å. We investigated several possible systematic errors that could have caused this poor fit: the value we have used for the interstellar reddening, the flux calibration of HUT, the timing of the 35-day cycle, and the subtraction of the background airglow spectrum.

If $0 < E_{B-V} < 0.05$, then a greater value of \dot{M} is required to fit the data. The higher resulting temperature of the heated disk and star can compensate for the spectral change introduced by the reddening. For $E_{B-V} = 0.05$, the model predicts an observed flux from 1000–1100Å that is $\approx 15\%$ greater than in the case with no reddening; however, the fit is still not good, and $\chi^2 = 1.59$.

Increasing the flux in the HUT spectrum by a factor of 2 to reflect some unknown flux calibration problem results in a better fit ($\chi^2 = 1.33$) and $\log \dot{M} = -8.48$, which is more typical of Her X-1. At $\phi = 0.41, 0.61$, $V = 13.4$. The spectrum predicted by this model is shown in Figure 5.

The 35-day cycle of Her X-1 does not repeat exactly (Baykal et al. 1993). Thus there is some uncertainty in our choice of ϕ_{35} , which determines the orientation of the accretion disk. If we

allow ϕ_{35} to vary as a free parameter, we find $\chi^2 = 1.28$ for the best-fit values $\phi_{35} = 0.15 \pm 0.01$, $\log \dot{M} = -8.85 \pm 0.01$. Although the fit is much improved, $\log \dot{M}$ is further out of the range of previous observations. Using this 35-day phase, more of the hot, central disk is visible, and so the flux at shorter wavelengths is increased. The uncertainty in extrapolating the 35-day ephemeris through ΔN cycles can be approximated as $0.9 \Delta N^{1/2}$ d (Baykal et al. 1993). The difference between the best-fit value of ϕ_{35} and that expected from the nearest reported X-ray turn-on is ≈ 8 d, or a deviation of $\approx 3\sigma$.

As described in §2, we subtracted from the Her X-1 spectrum a smooth model of the airglow spectrum based on a blank-sky observation. There is marginal evidence in the blank-sky spectrum for weak airglow lines of Ly δ , ϵ , γ near 930, 938, 950 Å, where our fit to the data is poor. We tested our method of background subtraction by smoothing the blank-sky spectrum with a Savitzsky-Golay filter. While this method introduces errors near the wings of the strong airglow lines, it can approximate the airglow background even when strong lines are not present. Using this method of background subtraction does not change our derived value of \dot{M} , and the model still predicts too low a flux below 1200 Å, but now $\chi^2 = 1.39$. Furthermore, this shows that there may be significant errors introduced by the background-subtraction.

In summary, we find that the Her X-1 far-UV spectrum was unusually faint at the time of our observation, resulting in model fits with values of \dot{M} lower than previously reported. The flux < 1200 Å is stronger than expected from detailed models. Uncertainties in the 35-day phase, the centering of Her X-1 in the aperture, or the background-subtraction may account for these discrepancies.

3.3. Analysis of the Emission Lines

We have compared the observed emission line fluxes with those predicted by theoretical models of X-ray illuminated accretion disks (Raymond 1993). The results are shown in Table 1. The “COS” model for the emission lines uses cosmic abundances, while the “CNO” model uses a fixed enhancement of He and N and a fixed depletion of C to represent abundances due to CNO processing. In computing the emission line strengths expected from the models, we have assumed that Her X-1 is at a distance of 5.5 kpc, and have made no correction for interstellar reddening.

The spectrum confirms the basic predictions of the X-ray illuminated accretion models. In particular, the interpretation of the NV/CIV ratio as an element abundance effect, rather than a problem with the predicted ionization or density structure, is borne out by the line strengths. While the NV $\lambda\lambda$ 1238.8, 1242.8 doublet is stronger than CIV $\lambda\lambda$ 1548.2, 1550.8, the OVI $\lambda\lambda$ 1031.9, 1037.6 lines may be slightly weaker. This supports the conclusion that the unexpected strength of the NV lines relative to CIV does not result from a dependence of line flux on ionization potential.

The presence of OVI emission lines in Her X-1 is interesting because OVI is formed in a

hotter region than any of the other UV lines. The ratio of O VI $\lambda\lambda$ 1031.9, 1037.6 to O V λ 1371 provides a temperature diagnostic. The O V line is produced from recombination of O VI and thus has the same dependence on the O VI ionization fraction and on the electron density as the O VI $\lambda\lambda$ 1031.9, 1037.6 lines. The strength of the O VI $\lambda\lambda$ 1031.9, 1037.6 lines depends on the strongly temperature-dependent excitation rate of the upper level of the transition. Using the O VI recombination rates of Nussbaumer & Storey (1984) and the standard excitation rate expressions and cross-section found in Osterbrock (1989), we find temperatures of $1.44 \pm 0.07 \times 10^4$ K and $1.48 \pm 0.07 \times 10^4$ K for the O VI $\lambda\lambda$ 1031.9, 1037.6 fluxes inferred assuming, respectively, a 2:1 doublet ratio and a 1:1 ratio with interstellar absorption. Correcting for reddening (using $E_{B-V} = 0.05$) increases O VI/O V by a factor of 1.44. This only increases the temperature estimate to 15,000 K.

HWb model the line emitting region, and for the N V region find $\log T = 4.44 \pm 0.02$, and $\log n = 13.24 \pm 0.06$, assuming a cosmic abundance of N and that all N is in the N V state. Our temperature estimate has assumed that the O VI $\lambda\lambda$ 1031.9, 1037.6 lines are optically thin; if this assumption is not right, then the temperature may be much higher. Further, we have assumed that the O VI lines and the O V line are emitted in the same regions or in regions with similar temperatures and densities, which may not be the case.

Both the COS model and the CNO model predict observable C III λ 977 emission (7.5×10^{-13} and 4.2×10^{-13} erg s $^{-1}$ cm $^{-2}$ respectively). The weak features that we saw had total flux $< 2.5 \times 10^{-13}$ erg s $^{-1}$ cm $^{-2}$. Interstellar C III λ 977 absorption would probably decrease the strength of this line by $\lesssim 20\%$. We note that Anderson et al. (1994) observed the C III λ 1175 line with HST (when the N V and C IV lines were twice as strong as observed with HUT), and found a flux of 2.7×10^{-13} erg s $^{-1}$ cm $^{-2}$, whereas COS and CNO predict fluxes of 1.0×10^{-12} and 4.6×10^{-13} erg s $^{-1}$ cm $^{-2}$, respectively. A further decrease in the C/N ratio beyond $C/N = 0.66$ as assumed in model CNO to $C/N = 0.5$ would improve the agreement between observations and models, but the evidence is not overwhelming.

This observation with the Hopkins Ultraviolet Telescope was the first to study the flux from this interesting source below the Lyman α line, where a large fraction the continuum emission probably arises in the disk, and where there are strong emission lines especially sensitive to X-ray illumination. Future observations with FUSE will be able to detect these features with greater sensitivity and resolution.

It is a pleasure to thank the many members of the HUT team at JHU and at the JHU Applied Physics Laboratory whose years of work paid off in two successful Astro missions. We also thank the Spacelab Operations Support group at Marshall Space Flight Center and the crew of the Astro-1 mission for their support before and during the flight. We would like to thank the referee, Ian Howarth, for a careful reading and for suggestions on improving the manuscript. The Hopkins Ultraviolet Telescope project is supported by NASA contract 5-27000 to The Johns Hopkins University. BB and SV were supported in part by NASA (NAG5-2532, NAGW-2685),

and NSF (DGE-9350074).

In this research, we have used, and acknowledge with thanks, data from the AAVSO International Database, based on observations submitted to the AAVSO by variable star observers worldwide.

Table 1: HUT Measurements of Emission Lines in Her X-1

Line	$\lambda_{\text{obs}}^{\text{a}}$ (\AA)	λ_{lab} (\AA)	FWHM(λ) (\AA)	Blueshift (km/s)	Flux ($\text{erg s}^{-1} \text{cm}^{-2}$)	COS ^b	CNO ^c	χ_{red}^2
O VI	1029.28 \pm 0.19	1031.93	3.60 \pm 0.36	770 \pm 60	7.1 \pm 0.7(-13)	1.8(-12)	8.9(-13)	78.3/44
O VI ^d	1029.12 \pm 0.14	1031.93	3.61 \pm 0.35	820 \pm 40	8.9 \pm 0.1(-13)			66.0/42
N V	1236.95 \pm 0.45	1238.82	8.7 \pm 2.6	450 \pm 110	8.3 \pm 1.0(-13)	4.7(-13)	5.9(-13)	29.6/35
C IV	1547.16 \pm 0.58	1548.20	7.0 \pm 1.4	200 \pm 110	3.27 \pm 0.51(-13)	1.03(-12)	5.3(-13)	94.1/94
O V	1369.23 \pm 0.18	1371.29	1.4 \pm 0.4	450 \pm 40	8.2 \pm 2.4(-14)	6.1(-14)	4.4(-14)	40.1/33
C III		977.02			< 2.5(-13)	7.5(-13)	4.2(-13)	

^aFor doublets, the wavelength given is the wavelength of the blue component.

^bModel with Cosmic abundances, from Raymond (1993), Table 2. The distance to Her X-1 is assumed to be 5.5 kpc.

^cModel with metal abundances enhanced due to CNO processing. From Raymond (1993).

^dAssuming an interstellar absorption line and an intrinsic 1:1 doublet ratio. The flux listed is the flux in the unabsorbed line.

REFERENCES

- Anderson, S.F., Wachter, S., Margon, B., Downes, R.A. 1994, *ApJ*, 436, 319
- Bahcall, J.N., & Bahcall, N.A. 1972, *ApJ*, 178, L1
- Baykal, A., Boynton, P.E., Deeter, J.E., & Scott, D.M. 1993, *MNRAS* 265, 347
- Blair, W. P., & Gull, T. R. 1990, *S&T*, 79, 591
- Boroson, B., Vrtilik, S.D., McCray, R., Kallman, T., & Nagase, F. 1996, *ApJ*, 473, 1079
- Boyle, S., Howarth, I., Wilson, R., & Raymond, J. 1986, in *ESA Proc. Int. Symp. on New Insights in Astrophysics*, 471
- Cheng, F.H., Vrtilik, S.D., & Raymond, J.C. 1995, *ApJ*, 452, 825
- Davidson, A. F., Henry, J. P., Middleditch, J., & Smith, H. E. 1972, *ApJ*, 177, L97
- Davidson, A. F. et al. 1992, *ApJ*, 392, 264
- Davies, S.R. 1990, *MNRAS*, 244, 93
- Deeter, J. E., Boynton, P. E., Miyamoto, S., Kitamoto, S., Nagase, F., & Kawai, N. 1991, *ApJ*, 383, 324
- Dupree, A. K., et al. 1978, *Nature*, 275, 400
- Feldman, P. F., et al. 1992, *Geophys. Res. Let.*, 19, 453
- Gerend, D., & Boynton, P. E. 1976, *ApJ*, 209, 562
- Giacconi, R., Gursky, H., Kellogg, E., Levinson, R., Schreier, E., & Tananbaum, H. 1973, *ApJ*, 184, 227
- Gruber, D. E., et al. 1980, *ApJ*, 240, L127
- Gursky, H., et al. 1980, *ApJ*, 237, 163
- Howarth, I. D., & Wilson, B. 1983a, *MNRAS*, 202, 347 (HWa)
- Howarth, I. D., & Wilson, B. 1983b, *MNRAS*, 204, 1091 (HWb)
- Kondo, Y., Van Flandern, T. C., & Wolff, C. L. 1983, *ApJ*, 273, 716
- Kruk, J.W., Kimble, R.A., Buss, R.H., Davidson, A.F., Durrance, S.T., Finley, D.S., Holberg, J.B., and Kriss, G.A. 1997, *ApJ*, 482, 546
- Kurucz, R.L. 1992, in *The Stellar Populations of Galaxies*, ed. B Barbuy & A. Renzini (Dordrecht: Kluwer), p. 225
- Longo, R., Stalio, R., Polidan, R. S., & Rossi, L. 1989, *ApJ*, 339, 478
- Meyer, F., & Meyer-Hofmeister, E. 1984, *A&A* 104, 35
- Middleditch, J. 1983, *ApJ*, 275, 278
- Middleditch, J., Puetter, R. C., & Pennypacker, C. R. 1985, *ApJ*, 292, 267

- Milgrom, M., & Salpeter, E. E. 1975, ApJ, 196, 589
- Nussbaumer, H., & Storey, P.J. 1984, A&AS, 56, 293
- Ögelman, H. 1987, A&A, 172, 79
- Osterbrock, D.E. 1989, *Astrophysics of Gaseous Nebulae and Active Galactic Nuclei* (Mill Valley,, California: University Science Books)
- Petterson, J.A. 1975, ApJ, 201, L39
- Raymond, J.C. 1993, ApJ, 412, 267
- Schandl, S., & Meyer, F. 1994, A&A 289, 149
- Seaton, M. J. 1979, MNRAS, 187, 73P
- Tananbaum, H. Gursky, H., Kellogg, E. M., Levinson, R., Schreier, E., & Giacconi, R. 1972, ApJ, 174, L143
- Voges, W., Pietsch, W., Reppin, C., Trumper, J., Kendziorra, E., & Staubert, R., 1982, ApJ, 263, 803
- Vrtilek, S.D., & Cheng, F.H. 1996, ApJ, 465, 915
- Wolff, C. L., & Kondo, Y. 1978, ApJ, 219, 605

Fig. 1.— Flux-calibrated HUT spectrum of Her X-1. The top curve shows the observed spectrum before airglow subtraction, smoothed over five pixels ($= 2.5\text{\AA}$) for display purposes. The bottom curve shows a smooth fit to a pure airglow spectrum obtained with the same slit but at a different time during the mission.

Fig. 2.— Observed HUT spectrum of Her X-1 after first-order removal of airglow. This spectrum has been smoothed over five pixels.

Fig. 3.— The observed HUT spectrum in the vicinity of O VI $\lambda\lambda 1031.9, 1037.6$, the locally scaled background airglow emission, and our fit to the airglow lines (bold).

Fig. 4.— Plots of Her X-1 emission lines showing fits to the doublet profiles as indicated in Table 1. a) O VI region; b) N V region; c) C IV region; and d) O V region. The data are shown unsmoothed. The vertical lines represent the rest wavelengths of the emission lines.

Fig. 5.— The UV continuum flux observed by HUT (smoothed over 7 pixels) compared with a power-law fit (dotted line, labelled “PL”), a model of an X-ray illuminated star and disk (solid line, labelled “Model”). We also show a model fit to twice the observed spectrum and then divided by 2 (dashed line) to show the effect of a possible underestimate of the true flux from Her X-1.

Figure 1

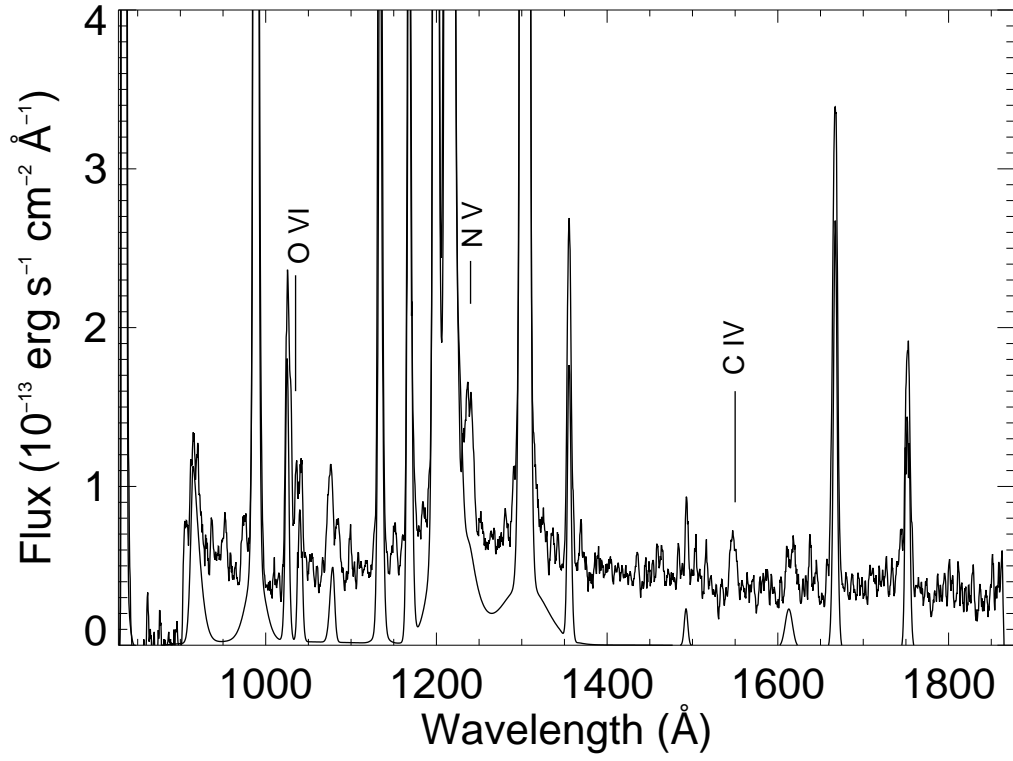


Figure 2

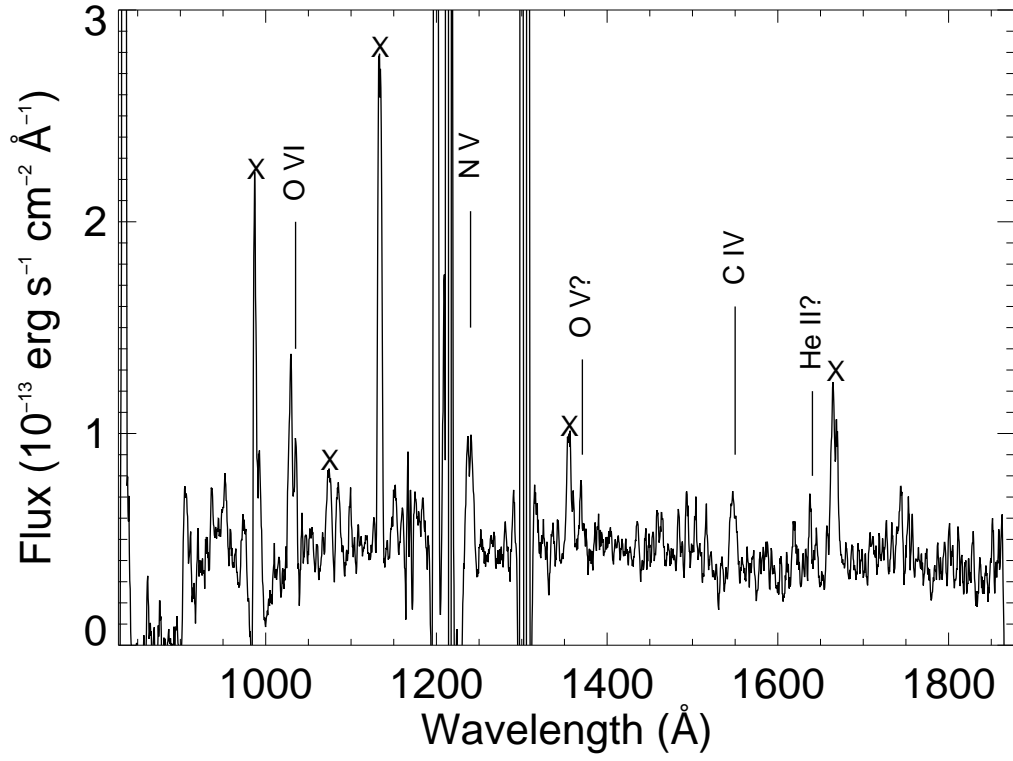


Figure 3

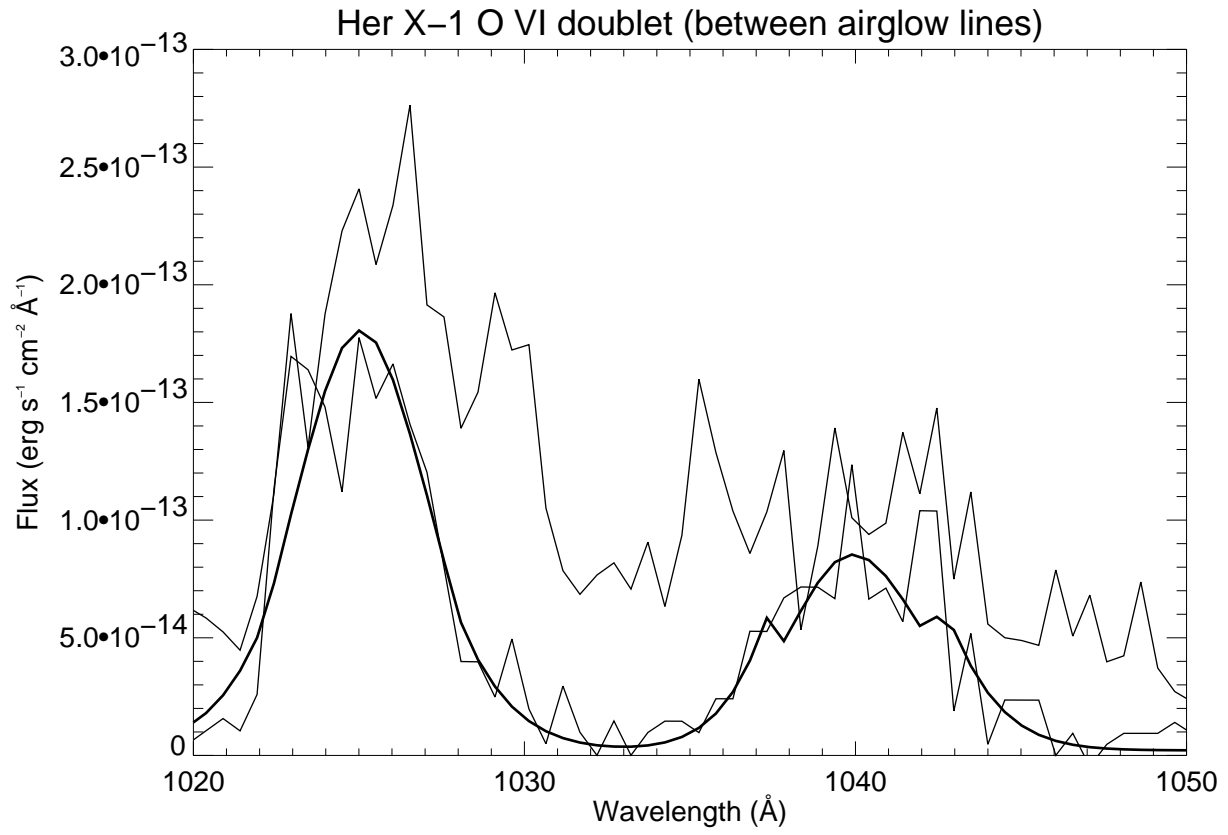


Figure 4

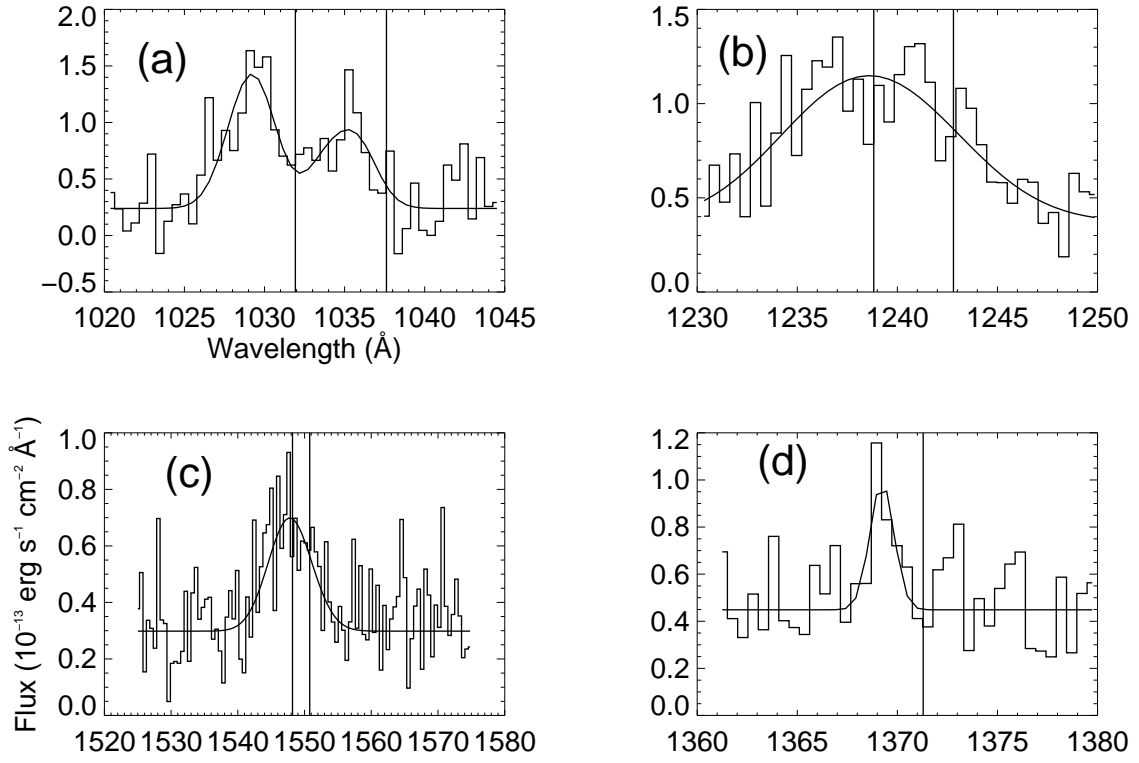


Figure 5

